Uncertainty in airflow rate estimation of daytime ventilation associated with atmospheric stability

Jongyeon Lim*, Ryozo Ooka, and Hideki Kikumoto

The University of Tokyo
4-6-1 Komaba, Meguro-Ku
Tokyo, Japan
**Corresponding author:jylim@iis.u-tokyo.ac.jp*

ABSTRACT

We conducted observations of wind velocity profiles above a high-density area in Tokyo, Japan, using a Doppler LIDAR system. Obtained data of the exponent index for the power law, which is commonly used to describe the wind velocity profile, displayed diurnal variation, decreasing in the daytime, which is expected in unstable atmospheric conditions. This paper provides information on the uncertainty in the calculated ventilation airflow rate due to the use of a constant value for the exponent index. The study was performed with data on wind pressure coefficients obtained from a numerical parametric study using computational fluid dynamics based on observation data. The uncertainty was assessed based on comparison of the ventilation airflow rate calculated using a constant value for the exponent index, and the ventilation airflow rate calculated considering a diurnal change in the exponent index. The results indicate that the ventilation airflow rate obtained from a constant value for the exponent index for an isolated building with two openings is underestimated by up to 8% in the daytime. A large relative uncertainty occurs at a lower height, i.e., a large relative error of the approaching wind velocity and a resulting error in the wind pressure coefficient.

KEYWORDS

Uncertainty analysis; ventilation performance; wind profile; power law; wind pressure coefficient.

1 INTRODUCTION

The local wind velocity affects the ventilation performance. Since the wind data in weather data files are usually measured at a meteorological station at a given height, the approaching wind velocity $U(z)$ for each height z of the building surface is modified from the measured meteorological wind velocity by Eq. (1), which is well known as the power law:

$$U(z) = U_n \left(\frac{z}{z_n} \right)^{\alpha} \tag{1}$$

where U_n [m/s] is the wind velocity at the height of the meteorological measurement z_n [m] and α [−] is the exponent index. It is common in engineering applications to describe the wind velocity profile using the power law because of its simplicity. The exponent index for the power law (α in Eq. (1)) is regarded to depend on ground roughness, and is taken to be constant. Several data sources have provided the relationship between α and terrain types, e.g., 0.22 for urban terrains, or 0.33 for towns and cities, as found in the ASHRAE Handbook (ASHRAE, 2001). However, these standard values are based on a predominant mechanical turbulence (very strong wind). Panofsky and Dutton (Panofsky and Dutton, 1984) noted that α

should be modified further when the contribution of convective turbulence becomes significant. This implies that the use of a constant value, e.g., 0.22 or 0.33 for α, contains an approximation error in calculating the approaching wind velocity when the effect of stratification becomes strong because of unstable atmospheric conditions. This error will contribute to the uncertainty in calculating the ventilation airflow rate Q [m^3/s], which is a function of wind velocity, as shown in Eq. (2),

$$Q = U_{ref} C_v A \sqrt{\Delta C_p} \tag{2}$$

where U_{ref} [m/s] is the reference wind velocity, which is often taken at the height of the rooftop in the free stream region, C_v [-] is the discharge coefficient of openings, A [m^2]is the area of the openings, and C_p [-] is the wind pressure coefficient.
The ventilation airflow rate is also a function of the wind pressure coefficient, which is defined as Eq. (3):

$$C_p = (P - P_0)/(\rho U_{ref}{}^2 / 2) \tag{3}$$

where P [Pa] is the static pressure at a given point on the building surface, P_0 [Pa] is the static reference pressure of the free stream, and ρ [kg/m^3] is the air density.
It is difficult to perform an accurate evaluation of C_p (Hensen, 1991) because of the various influencing parameters, including building configuration, details of the building surface, surrounding elements, and the characteristics of the approaching wind. Recently, with increasing application of computational fluid dynamics (CFD) to study the flow field around buildings, evidence where CFD has been used as a source of custom C_p data for building energy simulation has surfaced (Choi et al., 2012). However, when the inlet flow for a wind tunnel experiment or CFD is defined by the power law, the approximation error mentioned above, which results from using a constant α value, will also contribute to uncertainty in the C_p value. From Eq. (3) it is clear that C_p does not depend on the reference wind speed (U_{ref}), but the difference in α can cause changes in the approaching wind velocity profile, and subsequent changes in the wind pressure profile on the building surface. However, several studies have actually defined the inlet flow by the power law (Choi et al., 2012; Huang et al., 2007).
It can be concluded that the uncertainty of α effects the estimation of both U_{ref} and C_p values in Eq. (2), and consequently leads to uncertainty in calculation of the ventilation airflow rate Q in Eq. (2). This paper quantifies the uncertainty in the calculated wind-driven ventilation airflow rate due to diurnal changes in the approaching wind velocity profile. This diurnal variation is described by the fluctuation of the exponent index α for the power law, which is obtained from observations of the wind velocity profile using a Doppler LIDAR system (DLS).

2 OBSERVATION OF WIND VELOCITY PROFILE USING DOPPLER LIDAR SYSTEM

The wind velocity profile data used here were collected from a DLS (WindCube8, manufactured by LEOSPHERE) that was setup on the rooftop of the Institute of Industrial Science of the University of Tokyo, Japan (35°39'46"N, 139°40'41"E, 27.5 m altitude). The field of about 1-km radius surrounding the DLS is comparatively flat, and is mainly occupied by residential housing with varying heights of 3–9 m (73.8%), and a few buildings with heights over 30 m (0.5%). The mean height of the roughness elements is about 7 m, and the standard deviation of the heights of the roughness elements is about 4 m.

The observations were conducted from September 1, 2013 to June 30, 2014. The DLS used in this observation transmits a pulsed laser with a wavelength of 1.54 μm, receives the light backscattered by aerosols such as dust and other particles in the air, and measures the line-of-sight component of wind velocity using the Doppler frequency shift of the backscattered light. The orientation of transmission changes in the four cardinal directions, so that three components of wind velocity can be calculated. Using this DLS, the wind velocity data from 67.5 m to 527.5 m (20 m apart, 24 altitudes) were obtained with a temporal resolution of about 30 seconds.

The vertical component of measured wind velocity is one or more orders of magnitude smaller than the horizontal components. Hence, this analysis applies only to the horizontal components. We use wind velocity in this paper to refer to the scalar quantity of the horizontal velocity components. In inhomogeneous regions such as dense urban areas, the surrounding urban morphology often varies with direction, causing different wind profiles in each direction. However, in this paper, we discuss the wind profile obtained from the scalar quantities of the horizontal velocity components, without consideration of wind direction.

A total of about 3.5 million steps of data were obtained. Figure 1 shows the data acquisition ratio at each altitude for all observation periods, and for each month. The data acquisition ratio varies with altitude, with low data acquisition at low and high altitudes, and high data acquisition at medium altitudes. For data accuracy, we only used data obtained from time steps that had wind velocity data for all 24 altitudes. Furthermore, a large drop in the data acquisition ratio was found in winter, which we suggest is caused by the decrease in aerosol concentration. The overall data acquisition ratio was 40.9%.

Figure 3 shows the profiles of hourly averaged wind velocities and overall data, plotted on logarithmic axes. Each data point was normalized by z_{nDLS} and U_{nDLS}, which are the altitude with the highest data acquisition ratio (247.5 m) and the wind velocity at z_{nDLS}, respectively. Describing the wind velocity profile with a power law may be reasonable because linear relationships between velocity and altitude are apparent on the logarithmic axes. However, the wind profile varies by the hour. Since the slope of each line in Figure 3 corresponds to the exponent index for the power law (α in Eq. (1)), the value of α changes by the hour.

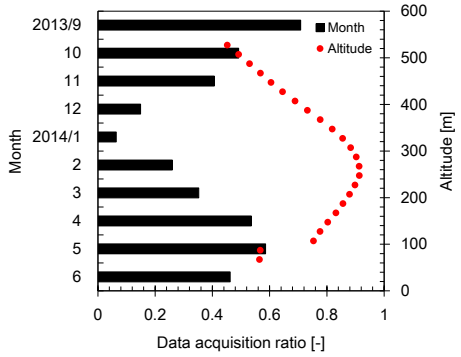

Figure 1: Data acquisition ratio at each altitude for all observation periods, and for each month.

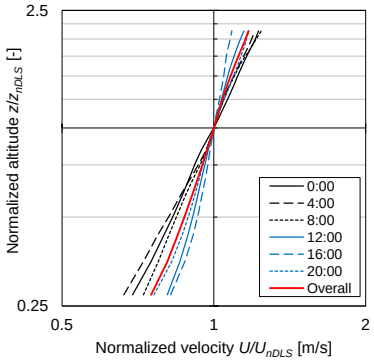

Figure 2: Mean profiles of hourly averaged and overall horizontal wind velocity.

Figure 3 shows the exponent index α derived from the mean profiles of hourly averaged and overall wind velocity data. Each value of α was calculated with a least squares error fit, which minimized the difference between the measured wind velocity at altitude z and $U(z)$ expressed by Eq. (1). The expected value of α for the study area is approximately 0.2 to 0.3, based on the terrain type. The exponent index α derived from the mean wind velocity profiles of all data in the observation period was 0.2, which is within the range. The values of α at night-time and early morning, which were expected to be neutrally stratified or stable, were also within the range. However, the values of α decreased to 0.1 in the daytime, displaying the

diurnal variation. This result is consistent with the previous observations (Touma, 1977; Farrugia, 2003), which reported that the value of α decreases under unstable atmospheric conditions. The effect of unstable stratification in the daytime is also suggested as a major factor in causing diurnal variation in our observations.

The fact that α decreases to 0.1 in the daytime can increase the uncertainty in the calculated daytime ventilation. This paper quantifies the uncertainty in the calculated ventilation airflow rate due to the use of a constant value as the exponent index α. The constant value used here is 0.22. In this paper, uncertainties in the calculated ventilation airflow rate for September 2013 and May 2014 in the observation period are presented and analysed in detail. The reasons for selecting May and September are outdoor air during these periods is considered to have high potential for natural ventilation, and the data acquisition ratio is higher than other periods, as shown in Figure 1.

Figure 4 shows diurnal changes in the exponent index and data acquisition ratio for September 2013 and May 2014. Although samples for September 2013 were larger than for May 2014, there are no significant differences between the hours for each month. Diurnal changes in the exponent index for both September 2013 and May 2014 are presented with the same aspect as for the exponent index derived from the profiles of hourly averaged wind velocity for the entire observation period (see Figure 3). The value of α decreased in the daytime in September 2013, displaying a minimum (α = 0.08) at 15:00 and a maximum (α = 0.31) at 23:00. We dealt with data from May 2014 (α = 0.07 at 14:00, and α = 0.39 at 06:00) in the same manner.

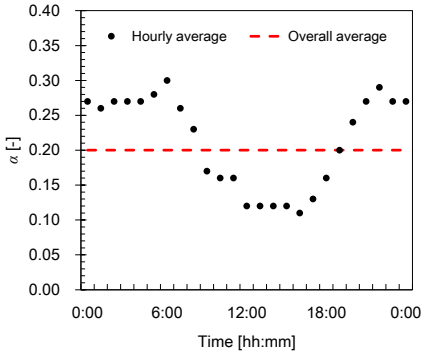

Figure 3: Exponent index derived from profiles of hourly mean and overall mean horizontal wind velocity.

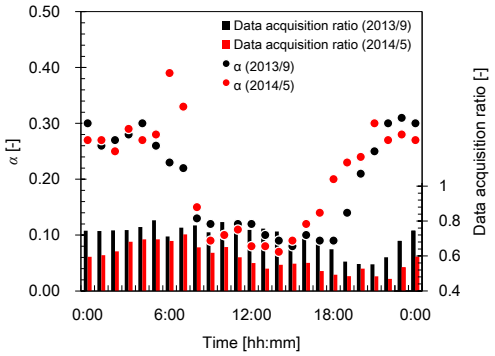

Figure 4: Exponent index derived from profiles of hourly averaged values and the data acquisition ratio in September 2013 and May 2014.

3 RESULTS

Ventilation performance is largely affected by conditions outdoors, such as wind velocity, which is usually obtained from weather data files. These data are modified using Eq. (1), and are used as the approaching wind velocity in building energy simulations. In this section, we present the uncertainties associated with using a constant value as the exponent index in such processes. To achieve this analysis, a 20-story building model with the dimensions 30 m (x) × 20 m (y) × 70 m (z) was designed. Although various weather data files have been generated to estimate building energy consumption, in this study we used the meteorological measurements of September 2013 and May 2014 in Tokyo because the exponent index data used in the analysis are the measured values for those periods. The uncertainties discussed in this section are uncertainties in the wind pressure coefficient on building surfaces, and the resulting uncertainty in the calculated ventilation airflow rate in the model building.

3.1 Relative wind pressure coefficient (C_p) error

In this section, the error of the value of C_p from using a constant value of α is quantified using comparisons with C_p values obtained using time-dependent values of α. The constant and time-dependent values of α used here are 0.22 and the observation result obtained from the DLS, respectively. We used the database from the computational parametric study using CFD as the C_p data source.

This study uses the parametric approach to obtain the C_p database with the designed building model. In the parametric study, cross-comparison of the effects of the diurnal wind profile variation is more easily achieved by observing changes in C_p on the building surface for different values of the exponent index α in the power law.

Five groups, comprising 23 values of α, are setup in five wind directions (0°, 22.5°, 45°, 67.5°, and 90°) and were simulated by the standard k-ε models. The α values were returned from the diurnal changes in α in Figure 4, but with no repetitions.

The building model is a 20-story building model as mentioned above. The size of the computational domain is 300 m (x) × 720 m (y) × 350 m (z). The total number of meshes was about 3,600,000, on a case-by-case basis. Tetrahedral meshes were employed, and finer meshes were arranged in the region near the building and ground surfaces, whereas the meshes were expanded farther away from the solid surface. The minimum mesh size near the building was 0.5 m. The inlet boundary condition was imposed by the power law as shown in Eq. (1), where U_n = 3.16 m/s, which is the averaged wind velocity during the two-month period (September 2013 and May 2014); z_n = 35.3 m, which is the height of the meteorological measurement for the data used; α was set to the above mentioned 23 values. We performed a total of 115 cases of CFD runs (23 values of α × five wind direction).

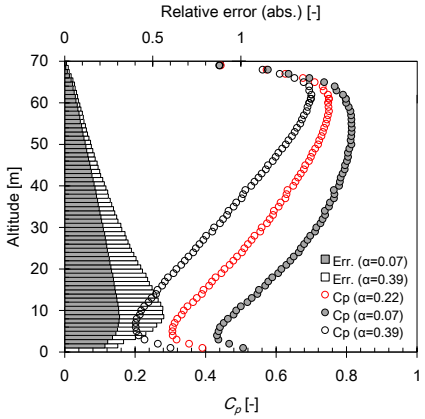

Figure 5: Vertical profile of C_p on windward surface for α = 0.07, 0.22, and 0.39, and relative errors.

Based on the CFD results, Figure 5 shows the vertical profile of C_p for the external wall on the windward side, where the wind is perpendicular to the south side of the building (0°), and the values of α for the inlet boundary are 0.07, 0.22, and 0.39. Each line probe has 69 data points spaced 1 m apart. The bar chart represents the relative error of C_p for α = 0.22 to that for α = 0.07 or 0.39. Using α = 0.22, C_p is underestimated when the value of α decreases under unstable atmospheric conditions. For α = 0.07, the relative C_p error reached 31%. In contrast, using α = 0.22 led to overestimation of C_p when the time-dependent values of α > 0.22. For α = 0.39, the relative C_p error reached 56%. The maximum error appeared at a height of about 10 m. Since the wind direction and the value of α vary by the hour, the calculation error is expected to vary with hour and altitude. Therefore, we estimated the root-mean-square error of ΔC_p ($RMSE_{CP}$) for hours and altitudes as defined in Eq. (4), where ΔC_p is the difference between the value of C_p on the windward and leeward surfaces:

$$RMSE_{CP}(t,z)=\sqrt{\frac{1}{D}\sum_{d=1}^{D}\left(\Delta C_p(d,t,z)_{\alpha=0.22}-\Delta C_p(d,t,z)_{\alpha=\alpha(t)}\right)^2} \tag{4}$$

where D is the day of a given month, $\Delta C_p(d, t, z)$ is ΔC_p for altitude z with the wind direction at hour t on the d^{th} day, obtained from the meteorological measurements for Tokyo, and $\alpha(t)$ is the time-dependent value of α at hour t, obtained from DLS observations. The value of $\Delta C_p(d, t, z)_{\alpha=0.22}$ is calculated using a constant value of α = 0.22, and $\Delta C_p(d, t, z)_{\alpha=\alpha(t)}$ is calculated using the time-dependent value $\alpha = \alpha(t)$.

Figure 6 shows the distribution of $RMSE_{CP}$ for September 2013 and May 2014. The value of ΔC_p was calculated based on the CFD result corresponding to the wind direction and the value of α at each hour. Based on data at 7:00 in September 2013 (see Figure 6(a)), since the value of α obtained from DLS observation was 0.22, $RMSE_{CP}$ was zero for all altitudes. However, at other times, the values of $\Delta C_p(d, t, z)_{\alpha=\alpha(t)}$ are different from ΔC_p $(d, t, z)_{\alpha=0.22}$, because $\alpha(t) \neq 0.22$, and such errors seem to be a function of altitude and hour. Larger values of $RMSE_{CP}$ were presented in the lower region of the building and in the daytime, i.e., large overestimation or underestimation in the calculated ΔC_p.

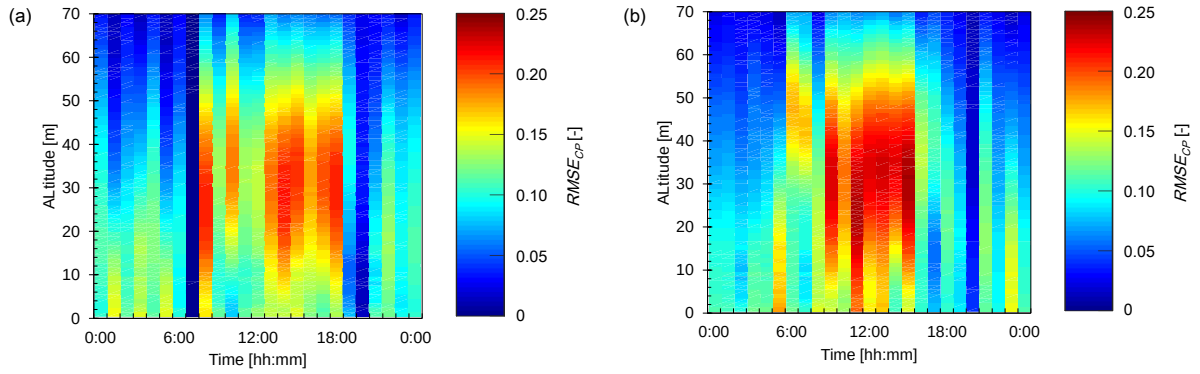

Figure 6: Estimation error of the wind pressure coefficient. (a) September 2013; (b) May 2014.

3.2 Uncertainty in the calculated ventilation airflow rate

In this section, the uncertainties in the calculated ventilation airflow rate are presented and analyzed in detail. To isolate the effects of the wind profile changes (i.e., the effect of the diurnal variation of α on the calculated ventilation airflow rate) from the effects of other parameters (e.g., characteristics of openings in the building), the building model was simplified. Drawing from Cóstola et al. (Cóstola et al., 2009), we designed a building model with the following assumptions: there is only one interior zone on each floor (no internal partitions); all floors have the same area and the same shape; there are only two openings for cross ventilation (no cracks in the external walls); all openings have the same area and the same discharge coefficient; buoyancy-driven ventilation is not considered.

Values of C_p on the face of each opening were obtained from our CFD database. We used surface-averaged C_p values of calculation grids corresponding to each opening. The ventilation airflow rate for each floor (1−20) was calculated using the C_p value obtained from the CFD database, and the approaching wind velocity was represented by a power law.

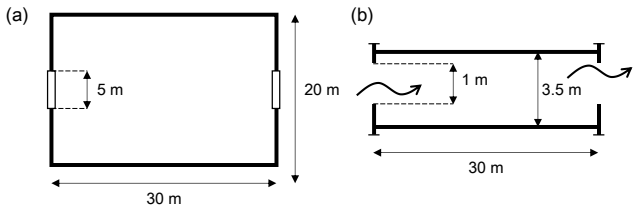

Figure 7: Geometry of a typical floor. (a) Floor plan; (b) cross section.

In this paper, only a situation with a pair of identical openings to achieve cross-ventilation was analyzed (see Figure 7). On each floor, ventilation is ensured by fully opened windows on the external walls, whose dimensions are 5 m × 1 m, and are characterized by a discharge coefficient of 0.7. The ventilation airflow rate was analyzed with the assumption that the pressure and velocity fields around the external walls are not changed by the presence of openings. Of course, depending on the size of the opening, it may significantly alter the pressure and velocity field in its vicinity. However, in this paper, we ignored the influence of the openings, and used the pressure and velocity field, which was determined in the absence of the opening, as boundary conditions for the airflow through the opening. In this case, the ventilation airflow rate (Q_{all}) can be calculated using Eq. (5):

$$Q_{all} = \sum_{f=1}^{20} Q_f = \sum_{f=1}^{20} U_{ref} C_v A \sqrt{\Delta C_p(f)} \tag{5}$$

where f is the floor number. In this paper, we regarded the ventilation airflow rate calculated by time-dependent α, $\alpha(t)$, as the "real" ventilation airflow rate. Therefore, the relative error of the ventilation airflow rate caused by the use of a constant value of $\alpha = 0.22$ is defined as Eq. (6):

$$E_{ACH}(t) = \frac{Q_{all}\big|_{\alpha=0.22} - Q_{all}\big|_{\alpha=\alpha(t)}}{Q_{all}\big|_{\alpha=\alpha(t)}} \tag{6}$$

Each term on the right side in Eq. (6) is a function of α, which affects $\Delta C_p(f)$ and U_{ref} in Eq. (5). It is clear that $E_{ACH}(t)$ does not depend on the opening characteristics (C_v and A). Despite the fact that the openings in the designed building model are somewhat unrealistic, the dependence of the characteristics vanishes when $E_{ACH}(t)$ is used in the process of estimating the uncertainties of the calculated ventilation airflow rate.

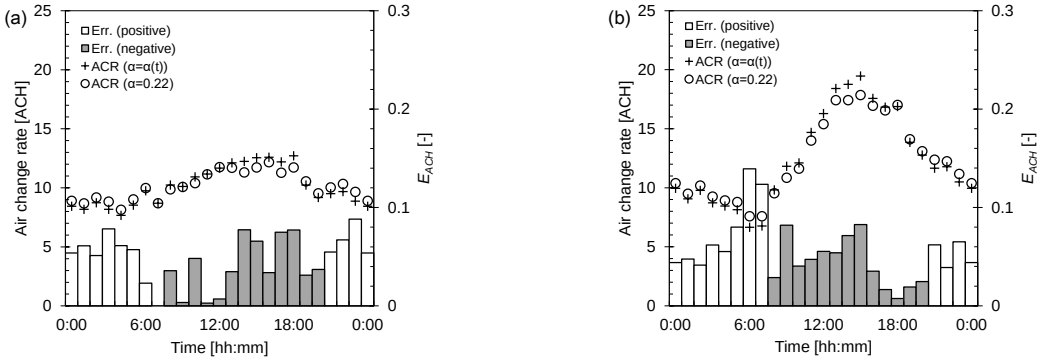

Figure 8: Calculated ventilation airflow rates and relative error. (a) September 2013 and (b) May 2014.

Figure 8 shows the calculated ventilation airflow rate Q_{all} converted to air change rate [ACH] and the relative error $E_{ACH}(t)$ for each hour. The air change rate tends to increase in the daytime because the wind velocities in the meteorological measurement data are higher in the daytime than at night. The magnitude of the relative error $E_{ACH}(t)$ varied by the hour, reaching about 14%, which is as large as the error from selecting C_p data sources. In addition, the air change rate was underestimated in the daytime and overestimated at night. Such results indicate that there may be no significant differences in the estimation of monthly overall ventilation performance in the case of 24-hour ventilation, i.e., underestimation in the daytime is at odds with overestimation at nighttime. However, several studies have investigated either daytime or nighttime ventilation (Choi et al., 2012; Ramponi et al., 2014). When C_p values derived from a constant value of α, determined only by terrain characteristics such as ground roughness, are used in such cases, the C_p error and resulting error of the ventilation airflow rate may be significant.

4 CONCLUSIONS

This paper presents an estimation of the uncertainty in the calculated ventilation airflow rate associated with changes in the wind velocity profile. Changes in the wind velocity profile are represented by a time-dependent exponent index for the power law, which is common in engineering application to describe the wind velocity profile. The ventilation airflow rate was calculated for a 20-story building model. The uncertainties that occurred in the process were quantified. The main conclusions are:

- From the observation of the wind velocity profile using a Doppler LIDAR system, we determined that the values of the exponent index for the power law were 0.2−0.3 in the nighttime and early morning, and decreased to 0.1 in the daytime, displaying a diurnal change. The exponent index derived from the mean wind velocity profiles of all data in the observation period was 0.2.
- The uncertainty in the estimated wind pressure coefficient corresponded to the exponent index. When the value of the exponent index was constant (0.22), the estimation accuracy was relatively high at nighttime, but the uncertainty became large in the daytime. Consequently, the estimation error for the ventilation performance varied by the hour, reaching about 14%, displaying a underestimation in the daytime and overestimation at night. The magnitude of the uncertainty is high, but the usability of these data depends on the problem, e.g., daytime and/or nighttime ventilation.

These results provide boundaries for further research on the wind pressure coefficient database. As a direction for improvement, we suggest classification by local climate and land use. Please refer to the main conclusions of the work.

5 ACKNOWLEDGEMENTS

A part of this study was supported by JSPS KAKENHI Grant Number 25-03368, 24226013, and 26709041. This financial contribution is highly appreciated.

6 REFERENCES

ASHRAE (2011). ASHRAE, ASHRAE handbook: fundamentals.

Choi, W., Joe, J., Kwak. Y., Huh, J. (2012). Operation and control strategies for multi-storey double skin facades during the heating season, *Energy and Buildings*, 49, 454–465.

Cóstola, D., Blocken, B., Ohba, M., Hensen, J. (2009). Uncertainty in airflow rate calculations due to the use of surface-averaged pressure coefficients, *Energy and Buildings*, 42, 881–888.

Farrugia, R. (2003). The wind shear exponent in a Mediterranean island climate, *Renewable Energy*, 28, 647–653.

Hensen, J. (1991). On the thermal interaction of building structure and heating and ventilating system, PhD thesis, Eindhoven University of Technology.

Huang, S., Li, Q., Xu, S. (2007) Numerical evaluation of wind effects on a tall steel building by CFD, *Journal of Constructional Steel Research*, 63, 612–627.

Panofsky, H., Dutton, J. (1985). *Atmospheric turbulence: models and methods for engineering applications.* New York: John Wiley & Sons.

Ramponi, R., Angelotti, A., Blocken, B. (2014). Energy saving potential of night ventilation: Sensitivity to pressure coefficients for different European climates, *Applied Energy*, 123, 185–195.

Touma, J. (1977). Dependence of the Wind Profile Power Law on Stability for Various Locations, *Journal of the Air Pollution Control Association*, 27, 863–866.